

# Surface-Enhanced Infrared Absorption: Pushing the Frontier for On-Chip Gas Sensing

Xinyuan Chong,<sup>1</sup> Yujing Zhang,<sup>2</sup> Erwen Li,<sup>1</sup> Ki-Joong Kim,<sup>3,5</sup> Paul R. Ohodnicki,<sup>3,4</sup> Chih-Hung (Alex) Chang<sup>2</sup> and Alan X. Wang<sup>1,\*</sup>

<sup>1</sup> School of Electrical Engineering and Computer Science, Oregon State University, Corvallis, OR 97331, USA

<sup>2</sup> School of Chemical, Biological and Environmental Engineering, Oregon State University, Corvallis, OR 97331, USA

<sup>3</sup> National Energy Technology Lab, United States Department of Energy, Pittsburgh, PA 15236, USA

<sup>4</sup> Materials Science and Engineering Department, Carnegie Mellon University, Pittsburgh, PA 15213, USA

<sup>5</sup> AECOM, P.O. Box 618, South Park, PA 15216, USA

\*Corresponding author: [wang@eecs.oregonstate.edu](mailto:wang@eecs.oregonstate.edu)

## Numerical Simulation

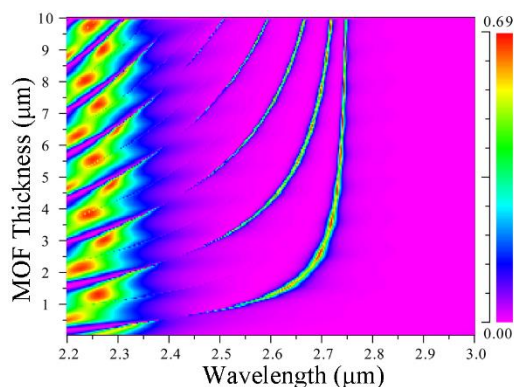


Figure S1. The scanning of MOF thickness.

The scanning of MOF thickness is shown in Figure S1, with all other parameters fixed. The color bar indicates the transmission intensity. The mode around 2.7  $\mu\text{m}$  is the mode  $M_t$  at the top Au/MOF/Air interface, which will be cutoff when the MOF thickness is less than 500 nm. As the thickness increases, more high-order modes will appear.

## Characterization

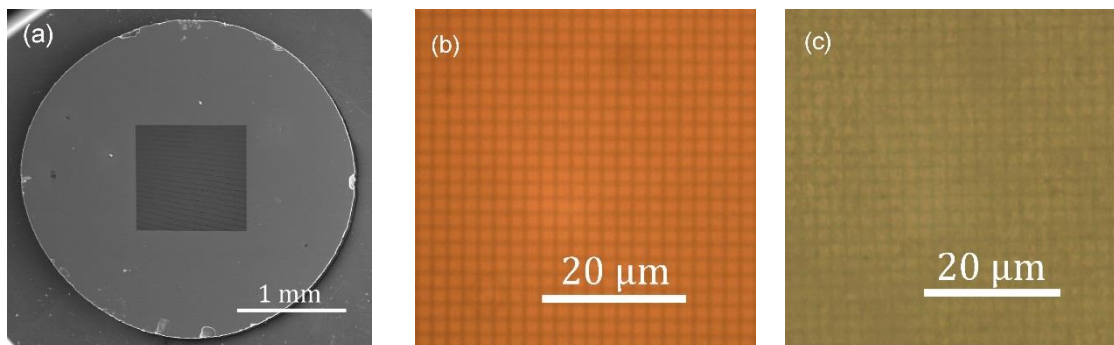


Figure S2. (a) The SEM image of the  $\text{Si}_3\text{N}_4$  nano-membrane on Si wafer. The optical images of Au-NPA (b) before and (c) after coating MOF.

The SEM image of  $\text{Si}_3\text{N}_4$  nano-membrane on Si wafer is shown in Figure S2 (a). The optical images of Au-NPA before and after coating MOF are shown in Figure S2 (b) and S2 (c).

## Experiment

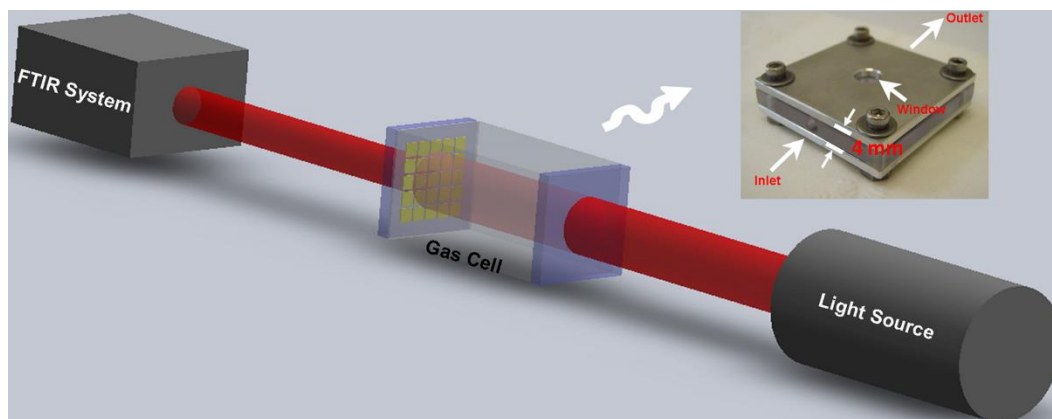


Figure S3. The schematic of the testing system with a home-made gas cell

The quantitative  $\text{CO}_2$  absorption measurement was performed by a commercial Fourier transform infrared (FTIR) spectrometer. A home-made gas cell was used in the test, which has 4 mm path length as shown in Figure S3. One side of the gas cell is sealed by a sapphire window and the other side is sealed by the device.

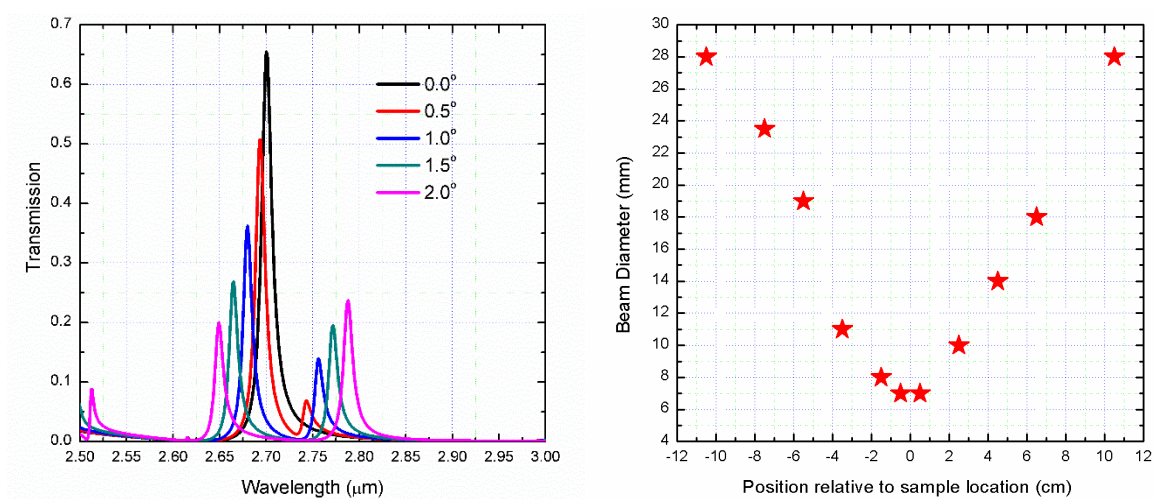


Figure S4. (a) The effect of incident angle deviation. (b) Beam diameter of FTIR.

The simulated transmission spectra of the device with different incident angles are shown in Figure S4 (a). We also measured the beam diameter of our commercial FTIR spectrometer. A tunable aperture was placed at different positions along the beam path. As shown in Figure S4 (b),

